*J Physiol* 588.6 (2010) pp 939–951



The Journal of Physiology

# Synchronized bursts of miniature inhibitory postsynaptic currents

Ion R. Popescu[1], Linda A. Morton[2], Alier Franco[1], Shi Di[1], Yoichi Ueta[3] and Jeffrey G. Tasker[1,2]

[1]*Department of Cell and Molecular Biology and* [2]*Neuroscience Program, Tulane University, New Orleans, LA, USA*
[3]*Department of Physiology, University of Occupational and Environmental Health, Kitakyushu, Japan*

**Spike-independent miniature postsynaptic currents are generally stochastic and are therefore not thought to mediate information relay in neuronal circuits. However, we recorded endogenous bursts of IPSCs in hypothalamic magnocellular neurones in the presence of TTX, which implicated a coordinated mechanism of spike-independent GABA release. IPSC bursts were identical in the absence of TTX, although the burst incidence increased 5-fold, indicating that IPSC bursts were composed of miniature IPSCs (mIPSCs), and that the probability of burst generation increased with action potential activity. IPSC bursts required extracellular calcium, although they were not dependent on calcium influx through voltage-gated calcium channels or on calcium mobilization from intracellular stores. Current injections simulating IPSC bursts were capable of triggering and terminating action potential trains. In 25% of dual recordings, a subset of IPSC bursts were highly synchronized in onset in pairs of magnocellular neurones. Synchronized IPSC bursts displayed properties that were consistent with simultaneous release at GABA synapses shared between pairs of postsynaptic magnocellular neurones. Synchronized bursts of inhibitory synaptic inputs represent a novel mechanism that may contribute to the action potential burst generation, termination and synchronization responsible for pulsatile hormone release from neuroendocrine cells.**

(Received 28 September 2009; accepted after revision 25 January 2010; first published online 1 February 2010)
**Corresponding author** J. G. Tasker: 2000 Stern Hall, Tulane University, New Orleans, LA 70118, USA.
Email: tasker@tulane.edu

**Abbreviations** aCSF, artificial cerebrospinal fluid; AP, action potential; ER, endoplasmic reticulum; mIPSC, miniature inhibitory postsynaptic current; MNC, magnocellular neurosecretory cell; mPSC, miniature postsynaptic current; OT, oxytocin; PSC, postsynaptic current; PVN, paraventricular nucleus; SON, supraoptic nucleus; VGCCs, voltage-gated calcium channels; VP, vasopressin.

## Introduction

Spike-independent, miniature postsynaptic currents (PSCs) are generally stochastic, and therefore their impact on postsynaptic action potential (AP) activity is limited to the effects of individual, stochastic PSCs or chance groupings of PSCs (Otsu & Murphy, 2003). In contrast, AP-evoked neurotransmitter release can be organized into bursts of PSCs by volleys of presynaptic APs, and these bursts can effect switch-like changes in the firing activity of postsynaptic neurones (Frost & Katz, 1996; Tadayonnejad *et al.* 2009). Neural circuits responsible for rhythmic outputs that result in stereotyped behaviours, such as locomotion and eating, can also employ bursts of AP-evoked PSCs to trigger or terminate postsynaptic AP bursting, and synchronized PSC bursts can impart synchronization to postsynaptic firing (Grillner & Matsushima, 1991; Frost & Katz, 1996; Marder & Bucher, 2007).

Exogenously applied neuromodulators, such as nicotine and serotonin, can cause bursts of miniature PSCs (mPSCs) in the absence of presynaptic AP activity (Sharma & Vijayaraghavan, 2003; Turner *et al.* 2004). Furthermore, venom-derived secretagogues, such as $\alpha$-latrotoxin, which has structural homology with the secretagogue hormones glucagon and pituitary adenylyl cyclase-activating peptide, also elicit mPSC bursts (Auger & Marty, 1997; Holz & Habener, 1998). This raises the possibility that AP burst generation and synchronization could be controlled in some cases by bursts of neurotransmitter release without the participation of presynaptic spiking. However, this would require the triggering of endogenous mPSC bursts at the appropriate time by afferent activity and synchronization of the mPSC bursts.

Pulsatile hormone release from neuroendocrine cells is an example of nervous system rhythmic output. The vasopressin- and oxytocin-secreting magnocellular neuroendocrine cells (MNCs) of the hypothalamus constitute a


DOI: 10.1113/jphysiol.2009.181461

model system of rhythmic output mediated by AP bursts, and, in the case of oxytocinergic cells, synchronized AP bursts (Brimble & Dyball, 1977; Belin *et al.* 1984; O'Byrne *et al.* 1986). Analysis of rat MNC spiking patterns *in vivo* indicates that AP bursts are influenced by synaptic inputs (Sabatier *et al.* 2004), and both glutamatergic and GABAergic neurotransmission are believed to contribute to AP bursting in the intact animal (Moos, 1995; Nissen *et al.* 1995; Voisin *et al.* 1995; Brown *et al.* 2004).

Here we report on endogenous bursts of mIPSCs in MNCs from acute slices that are caused by episodes of non-stochastic GABA release. The mIPSC bursts are calcium dependent and can trigger and terminate bursts of APs. IPSC bursts recorded when APs were not blocked were identical to mIPSC bursts, although they occurred with a higher incidence, suggesting that they are dependent on local afferent signalling. A subset of IPSC bursts were highly synchronized in onset in pairs of MNCs, suggesting a possible role of IPSC bursts in the synchronization of AP activity. Therefore, we propose that bursts of GABA release that are independent of presynaptic APs represent a potential mechanism of AP burst generation and synchronization.

## Methods

### Animals

Animals were group-housed under a 12 h light/dark cycle with *ad libitum* access to food and water. They were killed by decapitation under general anaesthesia by isoflurane inhalation. Hypothalamic slices, 300 $\mu$m in thickness and containing the supraoptic nucleus (SON) and/or the paraventricular nucleus (PVN), were prepared as previously described (Di *et al.* 2003). Procedures for animal handling were approved by the Tulane University Institutional Animal Care and Use Committee and were performed conformant with the Association for Assessment and Accreditation of Laboratory Animal Care (AAALAC) guidelines. Male, 5- to 12-week-old transgenic Wistar rats that express a vasopressin (VP)-enhanced green fluorescent protein (GFP) fusion gene were used in this study (Ueta *et al.* 2005). In these VP-GFP transgenic rats, VP neurones express enhanced GFP under the control of the VP promoter, causing them to fluoresce green under UV illumination. The recording of mIPSC and IPSC bursts from large numbers of GFP(+) and GFP(−) cells made it possible to ascertain their presence in both putative VP and oxytocin (OT) MNCs. Where only smaller numbers of cells were available, as in the case of cells receiving synchronous IPSC bursts, more data are needed for a reliable identification of the type(s) of MNC involved.

Experiments were conducted in MNCs primarily in the SON of male Wistar rats. Recordings in MNCs from female Wistar rats, from Sprague–Dawley rats and from MNCs in the PVN (identified based on previously defined criteria (Tasker & Dudek, 1991; Luther & Tasker, 2000) confirmed the presence of mIPSC bursts, but they were not included in the IPSC burst analysis.

### Electrophysiology

IPSCs were recorded in MNCs of the hypothalamic SON using the whole-cell patch-clamp technique in acute slices. They were recorded both as outward currents at a holding potential of 0 mV with electrodes containing (in mM): 110 D-gluconic acid, 110 CsOH, 10 CsCl, 10 Hepes, 1 $MgCl_2$, 1 $CaCl_2$, 11 EGTA, 2 Mg-ATP, 0.3 Na-GTP and 20 D-sorbitol (i.e. 'low [$Cl^-$] patch solution'), and as inward currents at a holding potential of −60 mV with electrodes containing (in mM): 120 CsCl, 30 Hepes, 2 $MgCl_2$, 1 $CaCl_2$, 11 EGTA and 4 ATP-Mg (i.e. 'high [$Cl^-$] patch solution'). The patch solution used for current-clamp recordings (described below) was also used for recording EPSCs in voltage clamp. The slices were submerged and perfused at a rate of 2 ml $min^{-1}$ with an artificial cerebrospinal fluid (aCSF) containing (in mM): 140 NaCl, 3 KCl, 1.3 $MgSO_4$, 1.4 $NaH_2PO_4$, 2.4 $CaCl_2$, 11 glucose, and 5 Hepes, which was bubbled with 100% $O_2$. Tetrodotoxin (TTX, 1 $\mu$M) was added to the perfusion bath to block $Na^+$-dependent APs when mIPSCs were recorded. In '$Ca^{2+}$-free' aCSF, $CaCl_2$ was replaced by 2 mM EGTA. MNCs were identified as VP neurones by direct visualization on a fixed-stage upright microscope (Olympus BX51W) using ultraviolet illumination and 488 nm/520 nm filters to detect GFP fluorescence, and GFP-positive and -negative neurones were then targeted for recordings using infrared illumination and differential interference contrast filters (IR-DIC) under transmitted light. Single and simultaneous paired recordings were made at 28°C with glass pipettes (1.2 mm i.d., 1.65 mm o.d., Garner, Claremont, CA, USA) of 3–8 MΩ resistance pulled in three stages on a P-97 horizontal puller (Sutter Instruments, Novato, CA, USA). We used a Multiclamp 700B amplifier and a Digidata 1322 digitizer controlled by pCLAMP9 software (Molecular Devices, Union City, CA, USA) to acquire intracellular data, which were stored on a computer hard disk. When testing the effect of TTX on AP-dependent IPSCs, recordings were made at a holding potential of 0 mV and a concentric bipolar stimulating electrode was placed in contact with the slice dorsal and adjacent to the ipsilateral optic chiasm at a distance of either ∼0.5 mm (half of the recordings) or ∼1.0 mm (half of the recordings) from the patch electrode. Single 0.5 ms pulses were generated by a Grass S48 stimulator (stimulus isolator model PSIU6), Grass Telefaktor, W. Warwick, RI, USA. For current-clamp recordings, the electrode solution contained (in mM): 140 potassium gluconate, 0.2 EGTA,

10 KCl, 10 Hepes, 3.5 sodium phosphocreatine, 4 Mg-ATP, 0.3 Na-GTP. A $[Ca^{2+}]$ of 0 mM in the pipette solution was used because this has been shown to promote AP bursting *in vitro* (Roper *et al.* 2004). Noradrenaline (5–10 $\mu$M) was added to the bath starting 20 min before testing to facilitate glutamate release, membrane depolarization and phasic firing (recurring bursts of APs) only in experiments involving spontaneous AP burst firing (Daftary *et al.* 1998). The membrane potential was not corrected for the junction potential in current-clamp recordings.

### Drugs

All drugs were purchased from Sigma (St Louis, MO, USA) or Tocris (Ellisville, MO, USA), except isoflurane (VetOne, Meridian, IN, USA). When testing the effects of DL-2-Amino-5-phosphonovaleric acid (APV) and 6-Cyno-7-nitroquinoxaline-2, 3-dione disodium salt (CNQX) (10 $\mu$M) or $Ca^{2+}$ on IPSC and mIPSC bursts, the initial solution was alternated between the control condition and the experimental condition to control for order- and time-dependent effects.

### Burst detection and quantification

Spontaneous IPSCs were selected using the template search function of Clampfit (pCLAMP9, Molecular Probes) and the MiniAnalysis 6.0 program (Synaptosoft). IPSC bursts were identified with the Clampfit Poisson Surprise protocol based on IPSC time of peak, yielding burst start and end times, and the surprise value. The Poisson Surprise is a measure of deviation from random (Poisson) distribution, and surprise values greater than 10 are generally accepted as indicative of bursts of APs or synaptic events (Legendy & Salcman, 1985; Kaneoke & Vitek, 1996). To our knowledge, no perfect algorithm exists for burst detection (Cocatre-Zilgien & Delcomyn, 1992). Therefore, for comparisons between drug conditions, we used these additional, empirically derived criteria: sudden burst onset, burst duration $>1.2$ s, and inter-event interval (IEI) $<200$ ms.

### Pre-recorded bursts of mIPSCs as stimulus templates

To approximate the effects of mIPSP bursts on AP activity, a digitally stored recording several seconds long containing periods of stochastically distributed mIPSCs flanking an mIPSC burst was used as a pCLAMP stimulus waveform template for the injection of DC current through the patch pipette in current-clamp recordings. The template current recording was acquired at a holding potential of 0 mV. The holding current and offset were digitally subtracted from the recorded current template to yield a 0 pA baseline, and the trace was multiplied by $-1$ to reverse the current direction (i.e. to produce a hyperpolarizing current template). The amplitude of the template file was scaled by 0.1, 0.2, 0.3. . .1 to produce the smallest effective amplitude that elicited a response in the different cells into which it was injected. We found it impractical to try to match the hyperpolarization elicited by the burst current injections with spontaneous IPSP bursts due to the low resolution of synaptic potentials in current-clamp recordings and the low incidence of IPSP bursts.

### Statistics

Paired two-sample *t* tests were used for within-cell comparisons, and two-sample *t* tests assuming equal variances were used for inter-cell comparisons. *P* values are based on two-tailed analyses unless stated otherwise. $P < 0.05$ was accepted as statistically significant. The Kolmogorov–Smirnov test was used to compare the amplitudes of burst and extra-burst mIPSCs. All values represent the mean $\pm$ the standard error of the mean.

## Results

### Bursts of mIPSCs

Bath application of 1 $\mu$M TTX completely abolished IPSCs evoked in MNCs of the SON by extracellular stimulation at a holding potential of 0 mV within 10 min ($n = 8$). In the same cells, the frequency of stochastic IPSCs was not affected by the TTX application ($1.27 \pm 0.23$ Hz *vs.* $1.27 \pm 0.27$ Hz, $n = 8$), as has been previously reported (Kabashima *et al.* 1997; Brussaard *et al.* 1999). The frequency of stochastic mIPSCs was significantly higher in GFP-negative, putative OT MNCs than in GFP-positive, putative VP MNCs ($1.41 \pm 0.11$ Hz *vs.* $0.84 \pm 0.2$ Hz, $P = 0.046$, $n = 7$, one-tailed), as has been previously reported (Li *et al.* 2007). Large clusters of high-frequency mIPSCs were recorded in MNCs in TTX and were identified as 'bursts' based on criteria described in the Methods. The mIPSC burst durations were in the range of seconds, intra-burst mIPSC frequencies were 10- to 100-fold higher than background frequencies, and bursts generally had a sudden onset and a gradual termination (Fig. 1*A*). The mIPSC bursts were observed in both GFP-positive, putative VP neurones and GFP-negative, putative OT neurones (Fig. 1*B*). Burst mIPSCs recorded at a holding potential of $-60$ mV had a decay time constant of $13.6 \pm 1.2$ ms ($n = 6$ cells displaying bursts recorded in 1 $\mu$M TTX, 50 $\mu$M APV and 10 $\mu$M CNQX). In contrast, mEPSCs had a decay time constant of $2.3 \pm 0.2$ ms ($n = 12$ cells recorded in TTX and 40 $\mu$M bicuculline methiodide) and were easily distinguished from mIPSCs. Miniature IPSC bursts occurred in 25% of neurones recorded for 30 min in TTX, whereas IPSC bursts (putative mIPSC

bursts) occurred in 57% of neurones recorded without TTX (see below).

The IPSC bursts consisted of $GABA_A$ receptor-mediated synaptic currents as they were abolished completely by 40 $\mu$M bicuculline methiodide in cells recorded at a holding potential of −60 mV (no TTX or APV/CNQX) in a within-cell comparison ($n = 10$). APV/CNQX tested at a holding potential of −60 mV in a within-cell comparison had no effect on the IPSC burst incidence (control *vs.* 50 $\mu$M APV/10 $\mu$M CNQX, $2.3 \pm 1.6$ *vs.* $3.2 \pm 1.1$ bursts $h^{-1}$, $n = 13$, 20 min in each condition), the burst duration ($2.2 \pm 0.4$ s *vs.* $3.3 \pm 1.1$ s), or the intra-burst IPSC frequency ($27.7 \pm 4.8$ Hz *vs.* $23.7 \pm 1.7$ Hz). The decay time constants of burst IPSCs were not different in the two conditions ($13.6 \pm 0.4$ ms *vs.* $14.8 \pm 0.7$ ms; $n = 4$ cells with bursts in the control condition and 7 cells with bursts in APV/CNQX). IPSC and IPSP bursts have been reported previously in MNCs in the absence of TTX (Andrew, 1987; Wang & Hatton, 2004).

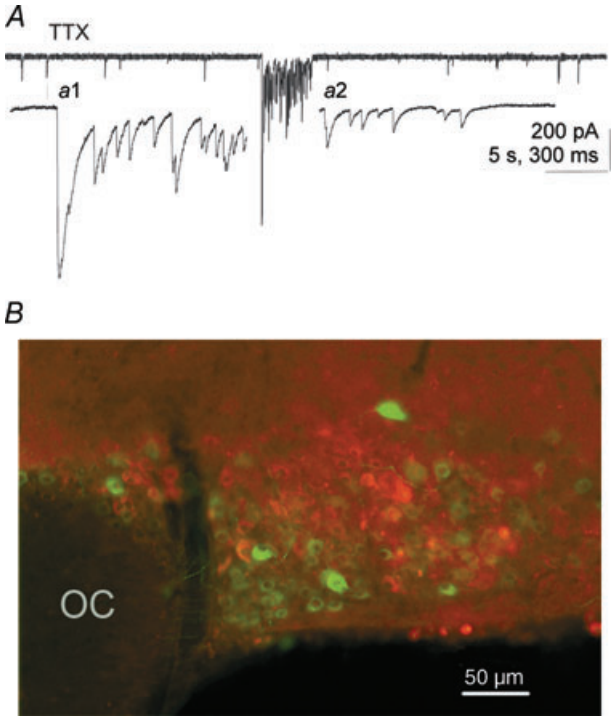


**Figure 1. mIPSC bursts in magnocellular neurones**
*A*, a representative example of an mIPSC burst recorded at −60 mV with a high [$Cl^-$] patch solution illustrating the typical abrupt onset with summated mIPSCs and the typical gradual termination. *a1* and *a2*, higher sweep speed details of the onset and termination of the burst in *A*. The external solution in *A* contained 1 $\mu$M TTX, 50 $\mu$M APV and 10 $\mu$M CNQX. *B*, mIPSC bursts were recorded from both putative VP and putative OT neurones (GFP+ and GFP−, respectively). The fluorescence micrograph demonstrates the GFP-specific labelling of VP neurones with an overlay of GFP-expressing VP neurones (green) and immunofluorescence-labelled OT neurones (red) in the same section of SON (monoclonal PS38 antibody to OT-neurophysin kindly supplied by Dr H. Gainer, National Institutes of Health, Bethesda, MD, USA). There was no detectable double labelling of neurones with the two markers. OC, optic chiasm.

Bursts of mIPSCs recorded in TTX were identical to bursts of spontaneous IPSCs recorded in the absence of TTX (Fig. 2*A–D*). We tested this in a within-cell comparison in which 11 cells were recorded for 30 min in control aCSF followed by 30 min in aCSF containing TTX. Five cells had bursts in both conditions. The burst duration ($3.2 \pm 0.4$ s without and $3.0 \pm 0.7$ s with TTX), intra-burst IPSC frequency ($32.1 \pm 6.1$ Hz without and $22.6 \pm 2.0$ Hz with TTX), and intra-burst IPSC decay time constant ($13.0 \pm 0.8$ ms without and $14.1 \pm 1.1$ ms with TTX) did not change in TTX, and the bursts were qualitatively indistinguishable in the two conditions. However, the IPSC burst incidence (i.e. bursts $h^{-1}$) was reduced 4-fold in TTX (from $4.5 \pm 1.9$ to $1.1 \pm 0.4$ bursts $h^{-1}$, $P = 0.025$, one-tailed), which suggested that the probability of IPSC burst generation is activity dependent. We also compared 54 cells recorded in control aCSF with another 72 cells recorded in TTX, each for 30 min. This inter-cell comparison revealed a similar identity of IPSC burst properties between bursts in control aCSF and those in aCSF with TTX, and a similar decrease in burst incidence in TTX (Fig. 2*E–G*). Thus, the burst duration ($2.4 \pm 0.1$ s and $2.7 \pm 0.2$ s, $n = 31$, 18) and the intra-burst IPSC frequency ($24.8 \pm 1.1$ Hz and $28.6 \pm 2.4$ Hz, $n = 31$, 18) did not change in TTX, whereas the burst incidence decreased over 5-fold in TTX ($8.2 \pm 1.6$ bursts $h^{-1}$ without TTX and $1.6 \pm 0.4$ bursts $h^{-1}$ with TTX, $n = 54$ and 72, $P = 0.00002$). The proportion of MNCs in the SON that displayed IPSC bursts also decreased in the presence of TTX. Thus, 31 of 54 neurones (57%) recorded in aCSF without TTX displayed IPSC bursts while 18 of 72 neurones recorded in aCSF with TTX (25%) displayed bursts. The variability of bursts across cells in this experiment is illustrated in Fig. 2*H*. The largest IPSC burst incidence we recorded was 260 $h^{-1}$ (no TTX). These data provide compelling evidence that the IPSCs within the bursts of both control and TTX-treated slices were not elicited by AP-dependent neurotransmitter release, but were caused by bursts of AP-independent GABA release. However, the probability of burst generation was activity dependent, since blocking AP activity with TTX decreased the incidence of bursts significantly.

### Calcium dependence of IPSC bursts

Calcium is a powerful catalyst of neurotransmitter release. Besides being necessary for AP-evoked neurotransmitter release (Katz & Miledi, 1965), extracellular $Ca^{2+}$ is also necessary for the mIPSC bursts elicited by serotonin and for at least part of the $\alpha$-latrotoxin-elicited release (Auger & Marty, 1997; Sudhof, 2001; Turner *et al.* 2004). We tested whether the GABA release responsible for mIPSC bursts observed in MNCs is $Ca^{2+}$ dependent. When the perfusion

medium was switched from aCSF containing APV, CNQX (no TTX) and normal $Ca^{2+}$ (2.4 mM) to aCSF containing APV, CNQX and 0 mM $Ca^{2+}$/2 mM EGTA (i.e. $Ca^{2+}$-free aCSF), all IPSC bursts disappeared ($3.4 \pm 1.4$ bursts $h^{-1}$ and 0 bursts $h^{-1}$, respectively; $n = 19$, $P = 0.021$, 20 min in each condition). In 3 of 6 cells that were recorded first in $Ca^{2+}$-free aCSF, bursts were only observed after switching to regular $Ca^{2+}$-aCSF with a latency >10 min. A similar result was obtained when the same experiment was performed in the presence of TTX (Fig. 3*A* and *F*). In this within-cell comparison, the mIPSC burst incidence was $2.1 \pm 1.0$ bursts $h^{-1}$ in normal aCSF and 0 bursts $h^{-1}$ in $Ca^{2+}$-free aCSF ($n = 13$, $P = 0.035$, one-tailed). Similar to the mIPSC burst incidence in these cells, we found that the frequency of background (extra-burst) mIPSCs was reduced in $Ca^{2+}$-free aCSF ($1.1 \pm 0.3$ Hz *vs.* $0.5 \pm 0.1$ Hz, $P = 0.007$, $n = 13$, in TTX, APV and CNQX) (Fig. 3*B* and *G*). In those cells in which recordings were started in normal aCSF, the mIPSC frequency was decreased from $1.3 \pm 0.5$ Hz to $0.5 \pm 0.1$ Hz ($P = 0.042$) when the perfusion was switched to the $Ca^{2+}$-free medium ($n = 7$). In cells recorded in $Ca^{2+}$-free medium first, the frequency increased when the perfusion was switched to normal $Ca^{2+}$ medium ($0.4 \pm 0.05$ Hz to $0.6 \pm 0.1$ Hz, $P = 0.031$, $n = 6$). Recording stability and input resistance ($1.1 \pm 0.1$ GΩ and $1.1 \pm 0.2$ GΩ) were not affected by the absence of extracellular $Ca^{2+}$. Therefore, GABA release responsible for mIPSC bursts as well as GABA release responsible for stochastic mIPSCs is $Ca^{2+}$ dependent.

Because intracellular $Ca^{2+}$ stores may become depleted when extracellular $Ca^{2+}$ is eliminated, we also tested if the $Ca^{2+}$ dependence of mIPSC bursts stemmed from $Ca^{2+}$ release from stores. A 30 min pre-incubation in thapsigargin (10 $\mu$M), a sarco(endo)plasmic reticulum $Ca^{2+}$-ATPase (SERCA) pump inhibitor that causes the depletion of $Ca^{2+}$ from the endoplasmic reticulum (ER), did not affect the incidence of mIPSC bursts during 30 min recordings (control cells, $1.7 \pm 1.3$ bursts $h^{-1}$, $n = 6$; thapsigargin-treated cells, $2.0 \pm 1.4$ bursts $h^{-1}$, $n = 10$, in TTX, Fig. 3*C*), suggesting that $Ca^{2+}$ release from intracellular stores is not required for mIPSC burst generation. Finally we tested for the involvement of voltage-gated $Ca^{2+}$ channels (VGCCs) in the generation of mIPSC bursts. Perfusing the slices with the VGCC blocker $Cd^{2+}$ (200 $\mu$M) had no effect on the incidence of mIPSC bursts (control cells, $1.3 \pm 0.9$ bursts $h^{-1}$, $n = 11$; $Cd^{2+}$-treated cells, $1.2 \pm 0.8$ bursts $h^{-1}$, $n = 10$, Fig. 3*D*). The amplitude of stochastic mIPSCs was not affected by the $Cd^{2+}$ treatment (control, $83.9 \pm 8.9$ pA, $Cd^{2+}$, $89.4 \pm 17.5$ pA, $n = 11$, 10, Fig. 3*E*), suggesting that no spurious interactions occurred between $Cd^{2+}$ and $GABA_A$ receptors. Therefore, the requirement of mIPSC bursts for extracellular $Ca^{2+}$ is not due to $Ca^{2+}$ influx through VGCCs.

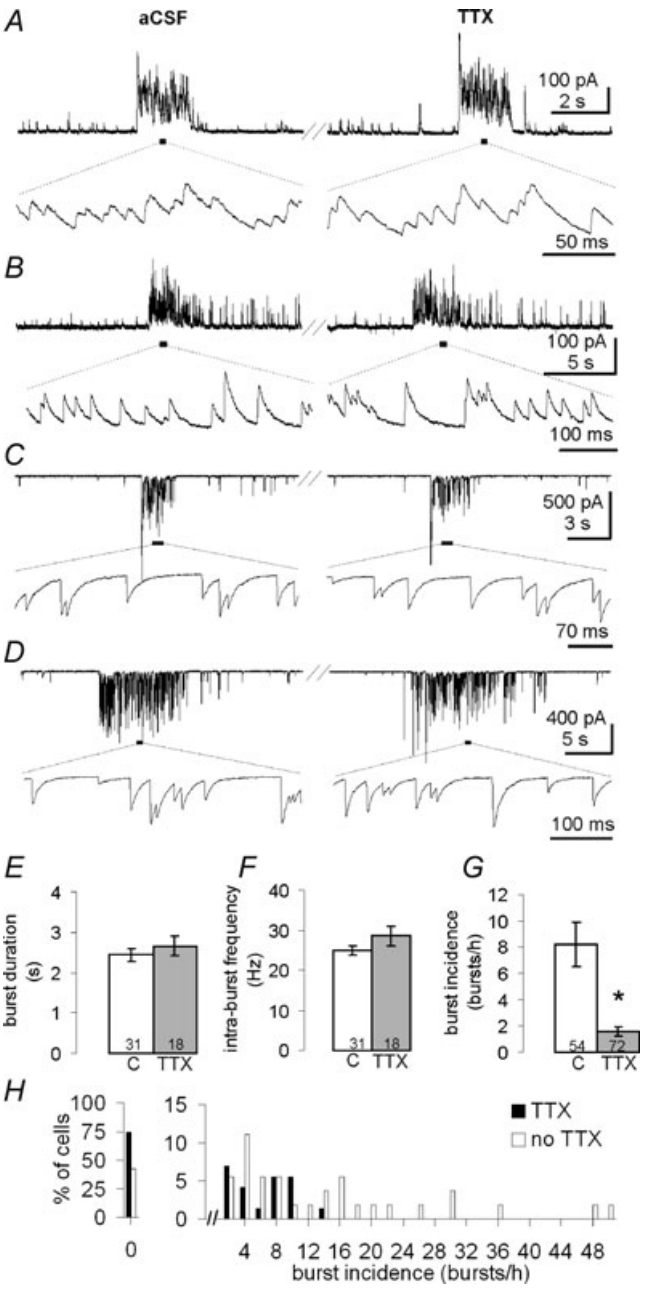


**Figure 2. IPSC bursts and mIPSC bursts are identical, except in incidence**

*A–D*, representative examples, from 4 cells, of IPSC and mIPSC bursts recorded in normal aCSF (left) and after >10 min in TTX (right) in the same cells. In *A* and *B*, holding potential ($V_H$) was 0 mV. In *C* and *D*, $V_H$ was −60 mV and a high [$Cl^-$] patch solution was used. Lower traces are higher sweep speed details of segments underlined above. The IPSC burst duration (*E*) and intra-burst IPSC frequency (*F*) were the same in control aCSF (C) and aCSF containing TTX (TTX). The incidence of the IPSC bursts (*G*), on the other hand, was 5-fold greater in aCSF lacking TTX. *H*, the distribution of IPSC bursts in the cells represented in *E–G* (*x*-axis bin size is 2 bursts $h^{-1}$).

### mIPSC burst origin

In order to assess whether the GABA release responsible for the mIPSC bursts was restricted to a subset of synapses, we analysed the rise times and amplitudes of mIPSCs and compared the intra-burst mIPSCs with the extra-burst mIPSCs. If the bursts were generated at a limited number of synapses, the intra-burst mIPSCs would be expected to be more homogeneous than the extra-burst, background mIPSCs, which presumably originate at synapses distributed throughout the dendritic tree. We analysed mIPSCs from six randomly selected bursts in six cells recorded either at 0 mV, the approximate reversal potential for mEPSCs, or at −60 mV in APV/CNQX, all in TTX. Only events arising from baseline were analysed (i.e. after complete decay of previous mIPSCs), which limited our analysis to a subset of the mIPSCs. The 10–90% rise time of intra-burst mIPSCs ($0.81 \pm 0.09$ ms) was significantly faster than that of an equal number of extra-burst mIPSCs immediately preceding the burst ($1.51 \pm 0.23$ ms, $P = 0.012$, $n = 6$) (Fig. 4*A*–*D*). The coefficient of variation (CV = standard deviation/mean) of the rise time of intra-burst mIPSCs ($0.36 \pm 0.09$) was significantly smaller than the CV of extra-burst mIPSCs ($0.63 \pm 0.07$, $P = 0.017$, $n = 6$), indicating a lower variance of intra-burst mIPSC rise times. All six cells analysed also had mean intra-burst mIPSC amplitudes that were larger than the mean extra-burst mIPSC amplitudes ($122.3 \pm 20.4$ pA *vs.* $64.0 \pm 11.1$ pA, $P = 0.003$). The amplitude CV was also smaller for intra-burst mIPSCs than for extra-burst mIPSCs ($0.32 \pm 0.04$ *vs.* $0.57 \pm 0.06$, $P = 0.004$). The amplitude of burst and extra-burst mIPSCs for the six cells combined was also different according to the Kolgomorov–Smirnov test ($P < 0.001$). The cumulative fraction distribution is illustrated in Fig. 4*E*. It is worth noting, however, that about 5% of mIPSC bursts overall were composed of mIPSCs with mean amplitudes that were smaller than the mean stochastic mIPSC amplitude. These results suggest that the majority of mIPSC bursts were generated at a subset of synapses that were located relatively proximal to the soma. However, it is also possible that the larger mIPSC amplitudes observed in most bursts were caused by multiquantal GABA release. The quantal analysis required to assess this possibility was hampered by the high frequency of mIPSCs in bursts, which resulted in extensive summation and a relatively small number of free-standing mIPSCs. The amplitude histograms of burst

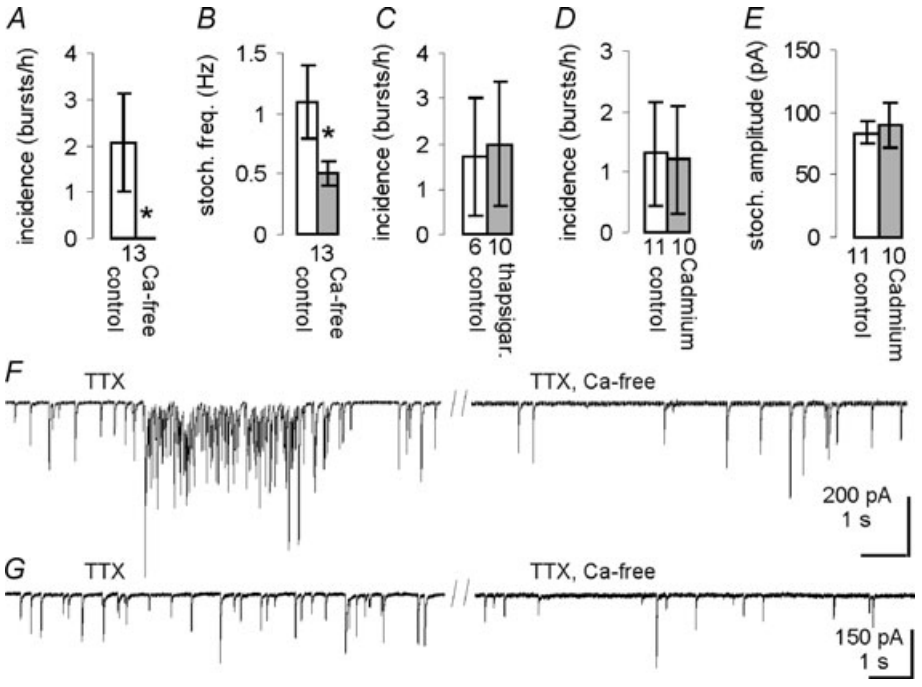


**Figure 3. The $Ca^{2+}$ dependence of mIPSC bursts and extra-burst mIPSCs**
Exchanging the normal extracellular medium with $Ca^{2+}$-free aCSF abolished all mIPSC bursts in a within-cell comparison (*A*) and in the same experiment also reduced the frequency of stochastic mIPSCs (*B*). Inhibiting the SERCA pump with 10 $\mu$M thapsigargin (*C*) or blocking VGCCs with 200 $\mu$M $Cd^{2+}$ (*D*) did not abolish the mIPSC bursts. *E*, the amplitude of background mIPSCs was not affected by $Cd^{2+}$. *F*, representative traces from one of the cells in *A* showing an mIPSC burst in normal aCSF (left, TTX) and the presence of only stochastic mIPSCs after 10 min of perfusion with $Ca^{2+}$-free medium (right, 'TTX, Ca-free'). *G*, representative traces from another of the cells in *A* illustrating the mIPSC frequency in normal aCSF (left) and after 20 min perfusion with $Ca^{2+}$-free medium (right).

and extra-burst mIPSCs for the cell with the longest burst duration are presented in Fig. 4*F*.

### The effect of mIPSP bursts on AP firing patterns

MNCs release their peptide hormones most efficiently during AP bursts (Dutton & Dyball, 1979). Therefore, we wanted to probe the effect of mIPSC bursts on AP firing patterns. A square hyperpolarizing current pulse (40–80 pA, 500 ms) applied at resting potentials close to threshold during an AP-free period was followed by a rebound depolarization in 11 of 34 cells. The rebound depolarization reached AP threshold and triggered spikes in 5 of these cells (Stern & Armstrong, 1995). When such pulses were given during a burst of APs, the burst was usually terminated, though sometimes several consecutive, contiguous pulses were required (1–6 contiguous pulses, $n = 16$ cells). To test the effects of a more physiological stimulus, we also used a burst of mIPSCs pre-recorded from a different neurone as a template for current stimulation delivered through the patch pipette ('mIPSC burst playback'). Neurones that responded to square hyperpolarizing pulses with rebound APs also generated APs in response to these mIPSC burst injections (Fig. 5*A*). In three of these neurones, the simulated mIPSP bursts triggered burst-like AP afterdischarges (Fig. 5*B* and *C*). When the mIPSC burst stimulus was delivered during a burst-like AP afterdischarge, it terminated the afterdischarge in 8 out of 10 cells (Fig. 6). Spontaneous bursts of IPSPs are more difficult to detect than IPSC bursts due to the relatively low resolution of synaptic events in current-clamp recordings. However, we recorded five cells in which the onset or the termination of trains of APs coincided with and appeared to be caused by spontaneous bursts of IPSPs (Fig. 7).

### Synchronized IPSC bursts

VP neurones and OT neurones respond to physiological stimuli with a shift in their firing pattern towards AP burst firing. Although the AP bursts in VP neurones are not known to be synchronized, the bursts are synchronized in OT neurones, resulting in the pulsatile release of OT into the blood circulation (Belin *et al.* 1984; O'Byrne *et al.* 1986). We looked for synchronized synaptic activity that might impart synchronization to the spiking of MNCs. In dual recordings in pairs of neurones that were $<100\,\mu$m apart, IPSC bursts with synchronized onsets were recorded in 7 of 28 pairs of neurones (25%) recorded for ~30 min per pair (Fig. 8). The time interval between IPSC burst onsets ranged from 0.6 ms to 27.6 ms (mean $= 6.1 \pm 3.7$ ms, $n = 9$ pairs of bursts). Individual IPSCs within synchronized IPSC bursts were not synchronized (Figs 8 and 9), indicating that gap junctions were not responsible for the synchronized IPSC bursts and supporting the notion that the IPSC bursts are spike independent. We did not detect any synchronous mIPSC bursts in 34 pairs of MNCs recorded in the presence of TTX (~30 min per pair).

Presynaptic GABA profiles forming synapses on two separate postsynaptic MNCs have been reported in electron microscopy studies, and the incidence of these 'shared' GABA synapses increases during lactation (Theodosis *et al.* 1981; Hatton & Tweedle, 1982; Gies & Theodosis, 1994). It has been hypothesized that shared

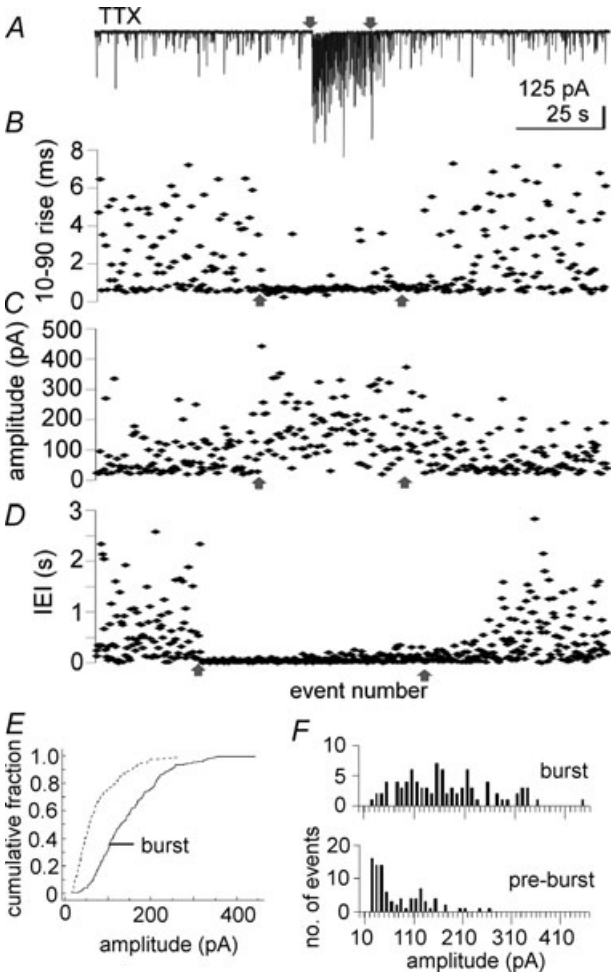


**Figure 4. Intra-burst mIPSCs have faster rise times and larger amplitudes than extra-burst mIPSCs**
*A*, recording of mIPSCs at −60 mV with high [$Cl^-$] patch solution. *B*,10–90% rise time; *C*, amplitude; and *D*, inter-event interval (IEI) of sequential mIPSCs immediately preceding, during and immediately following the mIPSC burst shown in *A*. Arrows indicate the same time points (the onset and end of the mIPSC burst). *x*-axis in *B–D* is event number. *B* and *C* contain only events with a flat baseline, whereas *D* contains the IEIs of all mIPSCs. *B–D* cover the same time periods. *E*, the cumulative fraction histogram for the amplitude of burst and background mIPSCs of all 6 cells analysed. *F*, the amplitude distribution of mIPSCs in the burst (top) and an equal number of mIPSCs preceding the burst illustrated in *A–D* did not reveal clear multiquantal events.

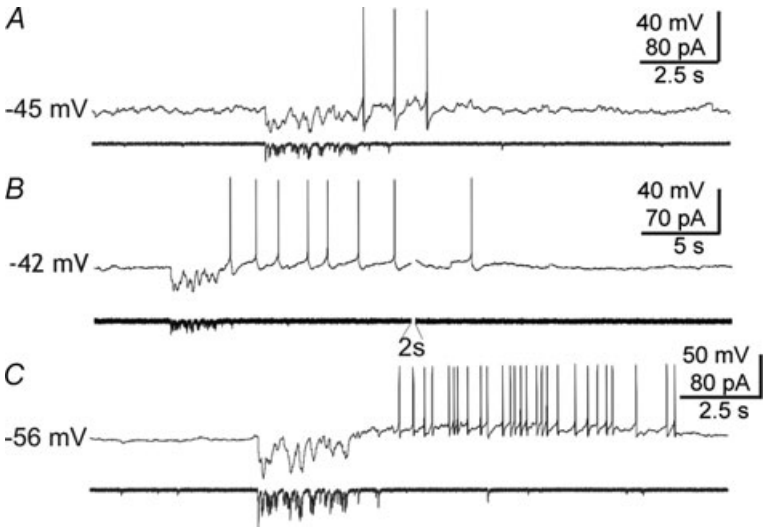


**Figure 5. Intracellular current injections mimicking an mIPSC burst triggered APs and AP afterdischarges**
*A*, an mIPSC burst current injection (lower trace) ('mIPSC burst playback', see Methods) triggered several APs. *B* and *C*, examples of cells responding to mIPSC burst current injections with AP afterdischarges. Upper traces are $V_m$ and lower traces $I_m$.

synapses may contribute to the synchronization of AP bursts in MNCs (Theodosis *et al.* 1981; Hatton & Tweedle, 1982). If the synchronized IPSC bursts described here originated at a single presynaptic bouton forming shared GABA synapses onto pairs of postsynaptic MNCs, they would be expected to be similar in duration and internal frequency. We tested for higher uniformity in the duration and frequency of the synchronized bursts compared to the unsynchronized bursts in dual recordings as evidence for synchronized IPSC burst generation at shared GABA synapses. The mean difference in burst duration for synchronized bursts was significantly smaller than the mean difference in burst duration for unsynchronized bursts ($0.32 \pm 0.07$ s and $0.77 \pm 0.14$ s, $P = 0.006$, $n = 6$ pairs) (Fig. 9). The mean difference in intra-burst IPSC frequency between synchronized bursts was not significantly different than the mean difference in intra-burst frequency between unsynchronized bursts ($13.7 \pm 4.8$ Hz and $20.2 \pm 8.4$ Hz, $P = 0.16$, one-tailed, $n = 6$). The higher homogeneity among the synchronized bursts' durations compared to the unsynchronized bursts' durations in paired recordings provides indirect support for the hypothesis that synchronized IPSC bursts are generated at shared synapses.

## Discussion

The main findings of this study are (1) that robust endogenous bursts of mIPSCs occur in hypothalamic magnocellular neurones, (2) that the mIPSC burst incidence is activity dependent and requires $Ca^{2+}$ influx via a VGCC-independent mechanism, and (3) that bursts of mIPSCs can be generated with a synchronous onset in pairs of magnocellular neurones.

The activity dependence of mIPSC burst incidence is indicated by the fact that IPSC bursts recorded in the absence of AP blockade were identical in duration and intra-burst frequency to mIPSC bursts, but they occurred with ~5-fold higher incidence. Therefore, we propose that IPSC and mIPSC bursts are manifestations of the same spontaneous (AP-independent) GABA release phenomenon. The decreased incidence of mIPSC bursts without a change in intra-burst frequency in the presence of TTX suggests that APs increase the probability of burst

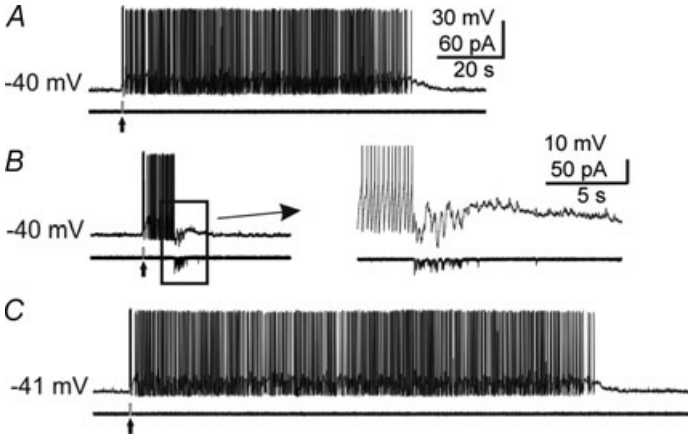


**Figure 6. Intracellular current injections mimicking an mIPSC burst terminated AP afterdischarges**
*A–C*, sequential records from one cell showing termination of a burst-like AP afterdischarge by an mIPSC burst current injection (see Methods). *A*, an intracellular DC depolarizing pulse (40 pA, 0.5 s, up-arrow) triggered 15 APs followed by a prolonged afterdischarge of APs. *B*, the same pulse was delivered and triggered an AP afterdischarge, but the burst was terminated by the injection of an mIPSC burst current injection during the AP afterdischarge. Inset: expanded view of boxed area. *C*, the depolarizing pulse was delivered again without the mIPSC burst current injection and again resulted in a prolonged AP afterdischarge. Upper traces are $V_m$ and lower traces $I_m$. Calibration bars in *A* also apply to *B* and *C* (except inset).

generation, although the clustered GABA release events comprising the bursts are AP independent.

The conclusion that spike-independent GABA release underlies IPSC bursts, including synchronized IPSC bursts, is further supported by the finding that onset-synchronized IPSC bursts did not contain individual IPSCs that were synchronized, other than the initial pair of currents. If the IPSCs within synchronized bursts were generated by AP-evoked neurotransmitter release from a common presynaptic neurone, then one would expect the IPSCs in both MNCs to be synchronized or phase locked by the presynaptic APs. On the other hand, individual IPSCs in the pair of postsynaptic cells would not be synchronized if neurotransmitter vesicle fusion did not occur in response to individual APs. Synchronized IPSC bursts could be generated in the classical way (one AP – one IPSC) in a polysynaptic circuit in which two GABA neurones were activated by a common afferent. This would allow for unsynchronized IPSCs within the IPSC bursts in the MNCs. However, the sub-millisecond difference in IPSC burst onset seen in some cases makes a polysynaptic synchronizing circuit unlikely.

The occurrence of IPSC bursts is both facilitated by AP activity and dependent on $Ca^{2+}$ availability. Our data indicate that extracellular $Ca^{2+}$ is necessary for mIPSC bursts. However, this requirement does not reflect the entry of $Ca^{2+}$ through $Cd^{2+}$-sensitive VGCCs or the release of $Ca^{2+}$ from thapsigargin-sensitive stores. Therefore, we hypothesize that $Ca^{2+}$-permeable ligand-gated channels, such as the nicotinic $\alpha$7 receptor or the serotonin 3 receptor, or $Ca^{2+}$-permeable pores, similar to those formed by $\alpha$-latrotoxin, may be the $Ca^{2+}$-entry paths responsible for clustered GABA release leading to mIPSC bursts. Further studies are required to test this hypothesis.

The TTX sensitivity and $Ca^{2+}$ dependence of IPSC burst generation point to the possibility of an extracellular messenger as a trigger that stimulates an increase in intracellular $Ca^{2+}$ to facilitate the flurry of GABA vesicle

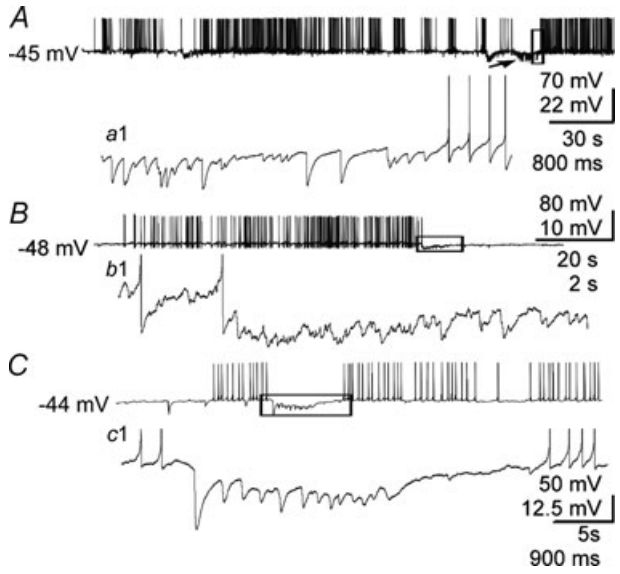


**Figure 7. Modulation of spiking activity by spontaneous IPSP bursts**
*A*, example of a spontaneous IPSP burst (arrow) that immediately precedes and appears to trigger a rebound burst of APs—a detail of which (of boxed area) is shown in (*a1*). *B*, example of a spontaneous IPSP burst that appears to terminate an AP burst-like afterdischarge. The afterdischarge of APs was triggered with a 0.5 s depolarizing pulse (as in Fig. 6). *b1*, detail of boxed area in *B* showing that the IPSP burst occurred at the end of the AP afterdischarge and appeared to contribute to its termination. *C*, another example of a spontaneous IPSP burst appearing to terminate a spontaneous train of APs. *c1*, detail of the boxed area in *C*, showing the IPSP burst between two spontaneous AP bursts and appearing to terminate the first of the two bursts.

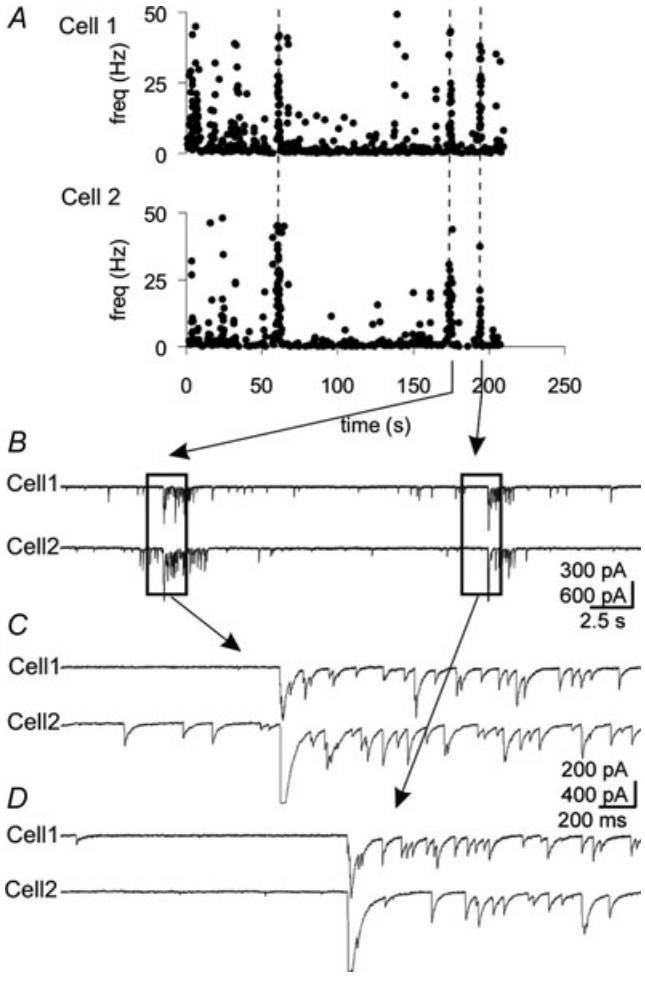


**Figure 8. Synchronized bursts of IPSCs in pairs of MNCs**
*A*, running histogram of frequency of IPSCs recorded simultaneously in 2 cells, spaced ~100 $\mu$m apart, at −60 mV with high [$Cl^-$] patch solution. Vertical dashed lines denote synchronized bursts. *B*, raw traces for portion of histogram in *A*, containing the last 2 episodes of synchronized bursts. *C* and *D*, expanded views of the left and right boxed areas in *B*, respectively.

fusions. The reliance of IPSC bursts on $Ca^{2+}$ influx via a non-VGCC-dependent mechanism supports the facilitation of IPSC burst generation by activation of a receptor. Another possible mechanism for the activity dependence of the IPSC bursts is priming of presynaptic axon terminals by APs. Thus, AP generation could create conditions in the presynaptic GABA terminals that increase the probability of $Ca^{2+}$-induced dumping of GABA vesicles.

Our analysis of the rise time and amplitude of mIPSCs in bursts suggests that they originated at a subset of synapses located proximal to the soma. Generation at a subset of synapses is suggested by the greater homogeneity (smaller CV) of the rise time and amplitude of mIPSCs in bursts compared to stochastic mIPSCs. The proximal origin of mIPSCs in bursts is suggested by their faster average rise times and greater average amplitudes than stochastic mIPSCs, consistent with less dendritic filtering. This proximal location may increase the mIPSP bursts' influence on the spiking activity of the MNCs. On the other hand, burst mIPSCs may generally have higher amplitudes because of an increase in the probability of multiquantal release during bursts. It was not possible in this study to perform the quantal analysis required to test this possibility because of the extensive summation of mIPSCs during the bursts. The amplitude histograms of burst and extra-burst mIPSCs do not suggest the presence of multiquantal events during the burst, but more examples of such extensive bursts will have to be recorded and analysed to test this hypothesis. A further possibility is that the differences in burst mIPSCs compared to background mIPSCs are due to mIPSC bursts being generated at synapses where a specific $GABA_A$ receptor subclass is prevalent.

The influence of mIPSP bursts on spiking is of interest because during birth, lactation or changes in plasma volume the MNC firing patterns shift towards AP bursts, thereby increasing the efficiency of hormone release (Brimble & Dyball, 1977; Dutton & Dyball, 1979; Belin *et al.* 1984; O'Byrne *et al.* 1986). Miniature IPSP bursts could affect AP bursts through mechanisms specific to the MNCs. Miniature IPSP bursts could trigger AP bursts in OT MNCs because hyperpolarizations and IPSPs trigger rebound depolarizations and APs in these neurones (Stern & Armstrong, 1995; Israel *et al.* 2008), including AP bursts (Armstrong *et al.* 1994), as is also the case in other types of neurones (Jahnsen, 1986; Llinás, 1988). The rebound depolarization is due to a sustained outward rectifying potassium current or to a low-voltage-activated $Ca^{2+}$ current (Stern & Armstrong, 1995; Israel *et al.* 2008). On the other hand, mIPSP bursts could cause AP burst termination in MNCs due to the collapse of the depolarizing plateau during spike suppression (Andrew & Dudek, 1984; Roper *et al.* 2004), or due to the removal of the inactivation of the MNCs' transient outward rectifying $K^+$ current by repolarizing the membrane potential below $\sim -55$ mV (Luther & Tasker, 2000). Miniature IPSC burst current injections resulted in depolarizations and AP bursts in quiescent neurones and AP burst termination in activated neurones. We also recorded spontaneous IPSP bursts occurring directly before and after spontaneous AP bursts, and after elicited AP bursts. Although it was not possible to determine precisely whether these IPSP bursts caused the subsequent generation or termination of AP trains, their incidence correlated with the corresponding shifts in activity.

OT neurones in the SON and PVN fire onset-synchronized AP bursts *en masse* during birth and

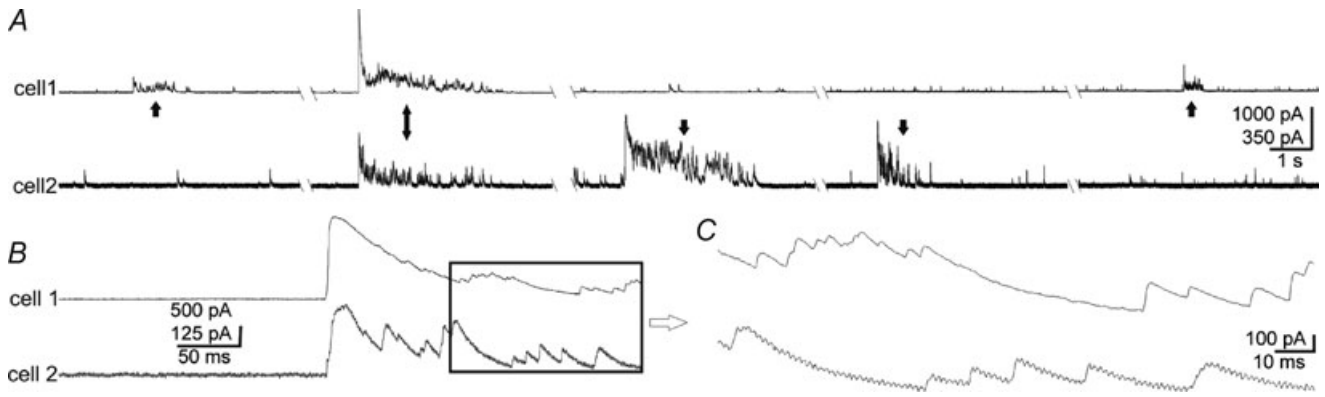


**Figure 9. Homogeneity of synchronized IPSC bursts**
*A*, example of synchronized bursts (double arrow, onset time difference 0.9 ms) recorded in a pair of MNCs at 0 mV with low $[Cl^-]$ patch solution and no TTX. Three sequential bursts are given for each cell, illustrating the similarity in duration for the synchronized bursts relative to the unsynchronized bursts. For cell 2, the first burst shown was the first burst of the recording. Unsynchronized bursts are indicated by single vertical arrows. *B*, the onsets of the synchronized bursts in *A* shown at higher sweep speed. *C*, detail of boxed area in *B* at higher sweep speed shows the IPSC resolution and also lack of synchronization of individual IPSCs.

lactation, producing a pulsatile output of OT (Poulain & Wakerley, 1982; Belin *et al.* 1984; O'Byrne *et al.* 1986). Although important advances have been made in understanding how afferent organization contributes to the synchronization of APs (Lincoln & Wakerley, 1975; Wang *et al.* 1997; Moos *et al.* 2004; Boudaba & Tasker, 2006), the synaptic mechanisms of synchronization are not fully understood. Synchronized EPSPs have been described in organotypic hypothalamic cultures (Israel *et al.* 2003), but not in acute slices. Electrotonic coupling between MNCs has also been reported (Hatton *et al.* 1988). However, we found no evidence for coupling in 62 recorded pairs of neurones. On the other hand, GABAergic neurotransmission has been shown to be necessary for the generation of milk ejection AP bursts in MNCs (Moos, 1995; Voisin *et al.* 1995), and GABA synapses are upregulated during pregnancy and lactation (Theodosis *et al.* 1995; Brussaard & Kits, 1999). The number of GABAergic synaptic specializations from single presynaptic boutons onto more than one postsynaptic target is also significantly increased in the SON during lactation (Theodosis *et al.* 1981; Hatton & Tweedle, 1982; Gies & Theodosis, 1994). These 'shared' GABA synapses provide a mechanism for synchronized postsynaptic GABA actions in multiple MNCs and have been postulated to function in MNC synchronization. We found bursts of IPSCs whose onsets were highly synchronized (mean onset difference $= 6.1 \pm 3.7$ ms). An analysis of synchronized and unsynchronized bursts in the same pairs of cells revealed a higher uniformity in burst duration and a trend towards higher uniformity in intra-burst frequency in synchronized bursts, which is consistent with generation at shared synapses. Onset-synchronized bursts of IPSPs would be expected to provide a strong synchronizing influence on AP bursting activity. Further experiments will be required to determine if synchronized IPSC bursts occur in both OT and VP neurones or in only one of these populations. It will also be worthwhile in the future to determine if the incidence of IPSC bursts and the incidence of their synchronization increase in tissue from lactating rats, since the incidence of shared GABA synapses increases with lactation.

We observed a low incidence of synchronized IPSC bursts ($\sim$0.6 bursts $h^{-1}$) in paired recordings made without AP blockade, and no synchronized bursts were detected in TTX. The low incidence of synchronized IPSC bursts is consistent with the lack of synchronized AP bursting activity observed in acute slices. If the bursts of quantal GABA release are facilitated by an extracellular messenger, then one would expect a low incidence of these bursts in the denervated *in vitro* slice preparation compared to the intact brain. It is not possible at this point to know whether the loss of synchronous IPSC bursts in the absence of APs is due to afferent blockade or to their lower incidence resulting in escape from detection. Synchronized IPSC bursts were observed in 25% of recorded cell pairs. In those pairs there was an average of 1.3 synchronized IPSC bursts. Considering that in TTX the incidence of mIPSC bursts was $\sim$5-fold lower and the percentage of cells displaying mIPSC bursts was $\sim$2-fold lower, escape from detection is likely.

Therefore, we present evidence that endogenous episodes of clustered, spike-independent GABA release occur in hypothalamic MNCs and that the incidence of these episodes is activity dependent. The resulting IPSC bursts can be closely synchronized and they can trigger and terminate AP bursts. These findings reveal a novel cooperativity in spontanous neurotransmitter release and present a potential mechanism for the generation and inter-neuronal synchronization of spiking activity in MNCs.

## References


Andrew RD (1987). Isoperiodic bursting by magnocellular neuroendocrine cells in the rat hypothalamic slice. *J Physiol* **384**, 467–477.

Andrew RD & Dudek FE (1984). Analysis of intracellularly recorded phasic bursting by mammalian neuroendocrine cells. *J Neurophysiol* **51**, 552–566.

Armstrong WE, Smith BN & Tian M (1994). Electrophysiological characteristics of immunochemically identified rat oxytocin and vasopressin neurones *in vitro*. *J Physiol* **475**, 115–128.

Auger C & Marty A (1997). Heterogeneity of functional synaptic parameters among single release sites. *Neuron* **19**, 139–150.

Belin V, Moos F & Richard P (1984). Synchronization of oxytocin cells in the hypothalamic paraventricular and supraoptic nuclei in suckled rats: direct proof with paired extracellular recordings. *Exp Brain Res* **57**, 201–203.

Boudaba C & Tasker JG (2006). Intranuclear coupling of hypothalamic magnocellular nuclei by glutamate synaptic circuits. *Am J Physiol Regul Integr Comp Physiol* **291**, R102–R111.

Brimble MJ & Dyball RE (1977). Characterization of the responses of oxytocin- and vasopressin-secreting neurones in the supraoptic nucleus to osmotic stimulation. *J Physiol* **271**, 253–271.

Brown CH, Bull PM & Bourque CW (2004). Phasic bursts in rat magnocellular neurosecretory cells are not intrinsically regenerative *in vivo*. *Eur J Neurosci* **19**, 2977–2983.

Brussaard AB, Devay P, Leyting-Vermeulen JL & Kits KS (1999). Changes in the properties and neurosteroid regulation of GABAergic synapses in the supraoptic nucleus during the mammalian female reproductive cycle. *J Physiol* **516**, 513–524.

Brussaard AB & Kits KS (1999). Changes in $GABA_A$ receptor-mediated synaptic transmission in oxytocin neurons during female reproduction: plasticity in a neuroendocrine context. *Ann N Y Acad Sci* **868**, 677–680.

Cocatre-Zilgien JH & Delcomyn F (1992). Identification of bursts in spike trains. *J Neurosci Methods* **41**, 19–30.

Daftary SS, Boudaba C, Szabo K & Tasker JG (1998). Noradrenergic excitation of magnocellular neurons in the rat hypothalamic paraventricular nucleus via intranuclear glutamatergic circuits. *J Neurosci* **18**, 10619–10628.

Di S, Malcher-Lopes R, Halmos KC & Tasker JG (2003). Nongenomic glucocorticoid inhibition via endocannabinoid release in the hypothalamus: a fast feedback mechanism. *J Neurosci* **23**, 4850–4857.

Dutton A & Dyball RE (1979). Phasic firing enhances vasopressin release from the rat neurohypophysis. *J Physiol* **290**, 433–440.

Frost WN & Katz PS (1996). Single neuron control over a complex motor program. *Proc Natl Acad Sci U S A* **93**, 422–426.

Gies U & Theodosis DT (1994). Synaptic plasticity in the rat supraoptic nucleus during lactation involves GABA innervation and oxytocin neurons: a quantitative immunocytochemical analysis. *J Neurosci* **14**, 2861–2869.

Grillner S & Matsushima T (1991). The neural network underlying locomotion in lamprey – synaptic and cellular mechanisms. *Neuron* **7**, 1–15.

Hatton GI & Tweedle CD (1982). Magnocellular neuropeptidergic neurons in hypothalamus: increases in membrane apposition and number of specialized synapses from pregnancy to lactation. *Brain Res Bull* **8**, 197–204.

Hatton GI, Yang QZ & Smithson KG (1988). Synaptic inputs and electrical coupling among magnocellular neuroendocrine cells. *Brain Res Bull* **20**, 751–755.

Holz GG & Habener JF (1998). Black widow spider $\alpha$-latrotoxin: a presynaptic neurotoxin that shares structural homology with the glucagon-like peptide-1 family of insulin secretagogic hormones. *Comp Biochem Physiol B Biochem Mol Biol* **121**, 177–184.

Israel JM, Le Masson G, Theodosis DT & Poulain DA (2003). Glutamatergic input governs periodicity and synchronization of bursting activity in oxytocin neurons in hypothalamic organotypic cultures. *Eur J Neurosci* **17**, 2619–2629.

Israel JM, Poulain DA & Oliet SH (2008). Oxytocin-induced postinhibitory rebound firing facilitates bursting activity in oxytocin neurons. *J Neurosci* **28**, 385–394.

Jahnsen H (1986). Electrophysiological characteristics of neurones in the guinea-pig deep cerebellar nuclei *in vitro*. *J Physiol* **372**, 129–147.

Kabashima N, Shibuya I, Ibrahim N, Ueta Y & Yamashita H (1997). Inhibition of spontaneous EPSCs and IPSCs by presynaptic $GABA_B$ receptors on rat supraoptic magnocellular neurons. *J Physiol* **504**, 113–126.

Kaneoke Y & Vitek JL (1996). Burst and oscillation as disparate neuronal properties. *J Neurosci Methods* **68**, 211–223.

Katz B & Miledi R (1965). The effect of calcium on acetylcholine release from motor nerve terminals. *Proc R Soc Lond B Biol Sci* **161**, 496–503.

Legendy CR & Salcman M (1985). Bursts and recurrences of bursts in the spike trains of spontaneously active striate cortex neurons. *J Neurophysiol* **53**, 926–939.

Li C, Tripathi PK & Armstrong WE (2007). Differences in spike train variability in rat vasopressin and oxytocin neurons and their relationship to synaptic activity. *J Physiol* **581**, 221–240.

Lincoln DW & Wakerley JB (1975). Factors governing the periodic activation of supraoptic and paraventricular neurosecretory cells during suckling in the rat. *J Physiol* **250**, 443–461.

Llinás RR (1988). The intrinsic electrophysiological properties of mammalian neurons: insights into central nervous system function. *Science* **242**, 1654–1664.

Luther JA & Tasker JG (2000). Voltage-gated currents distinguish parvocellular from magnocellular neurones in the rat hypothalamic paraventricular nucleus. *J Physiol* **523**, 193–209.

Marder E & Bucher D (2007). Understanding circuit dynamics using the stomatogastric nervous system of lobsters and crabs. *Annu Rev Physiol* **69**, 291–316.

Moos F, Marganiec A, Fontanaud P, Guillou-Duvoid A & Alonso G (2004). Synchronization of oxytocin neurons in suckled rats: possible role of bilateral innervation of hypothalamic supraoptic nuclei by single medullary neurons. *Eur J Neurosci* **20**, 66–78.

Moos FC (1995). GABA-induced facilitation of the periodic bursting activity of oxytocin neurones in suckled rats. *J Physiol* **488**, 103–114.

Nissen R, Hu B & Renaud LP (1995). Regulation of spontaneous phasic firing of rat supraoptic vasopressin neurones *in vivo* by glutamate receptors. *J Physiol* **484**, 415–424.

O'Byrne KT, Ring JP & Summerlee AJ (1986). Plasma oxytocin and oxytocin neurone activity during delivery in rabbits. *J Physiol* **370**, 501–513.

Otsu Y & Murphy TH (2003). Miniature transmitter release: accident of nature or careful design? *Sci STKE* **2003**, pe54.

Poulain DA & Wakerley JB (1982). Electrophysiology of hypothalamic magnocellular neurones secreting oxytocin and vasopressin. *Neuroscience* **7**, 773–808.

Roper P, Callaway J & Armstrong W (2004). Burst initiation and termination in phasic vasopressin cells of the rat supraoptic nucleus: a combined mathematical, electrical, and calcium fluorescence study. *J Neurosci* **24**, 4818–4831.

Sabatier N, Brown CH, Ludwig M & Leng G (2004). Phasic spike patterning in rat supraoptic neurones *in vivo* and *in vitro*. *J Physiol* **558**, 161–180.

Sharma G & Vijayaraghavan S (2003). Modulation of presynaptic store calcium induces release of glutamate and postsynaptic firing. *Neuron* **38**, 929–939.

Stern JE & Armstrong WE (1995). Electrophysiological differences between oxytocin and vasopressin neurones recorded from female rats *in vitro*. *J Physiol* **488**, 701–708.

Sudhof TC (2001). $\alpha$-Latrotoxin and its receptors: neurexins and CIRL/latrophilins. *Annu Rev Neurosci* **24**, 933–962.

Tadayonnejad R, Mehaffey WH, Anderson D & Turner RW (2009). Reliability of triggering postinhibitory rebound bursts in deep cerebellar neurons. *Channels (Austin)* **3**, 149–155.

Tasker JG & Dudek FE (1991). Electrophysiological properties of neurones in the region of the paraventricular nucleus in slices of rat hypothalamus. *J Physiol* **434**, 271–293.

Theodosis DT, el Majdoubi M, Gies U & Poulain DA (1995). Physiologically-linked structural plasticity of inhibitory and excitatory synaptic inputs to oxytocin neurons. *Adv Exp Med Biol* **395**, 155–171.

Theodosis DT, Poulain DA & Vincent JD (1981). Possible morphological bases for synchronisation of neuronal firing in the rat supraoptic nucleus during lactation. *Neuroscience* **6**, 919–929.

Turner TJ, Mokler DJ & Luebke JI (2004). Calcium influx through presynaptic 5-$HT_3$ receptors facilitates GABA release in the hippocampus: *in vitro* slice and synaptosome studies. *Neuroscience* **129**, 703–718.

Ueta Y, Fujihara H, Serino R, Dayanithi G, Ozawa H, Matsuda K, Kawata M, Yamada J, Ueno S, Fukuda A & Murphy D (2005). Transgenic expression of enhanced green fluorescent protein enables direct visualization for physiological studies of vasopressin neurons and isolated nerve terminals of the rat. *Endocrinology* **146**, 406–413.

Voisin DL, Herbison AE & Poulain DA (1995). Central inhibitory effects of muscimol and bicuculline on the milk ejection reflex in the anaesthetized rat. *J Physiol* **483**, 211–224.

Wang YF & Hatton GI (2004). Milk ejection burst-like electrical activity evoked in supraoptic oxytocin neurons in slices from lactating rats. *J Neurophysiol* **91**, 2312–2321.

Wang YF, Negoro H & Honda K (1997). Effect of interhemispheric sections of the hypothalamus on milk-ejection bursts of supraoptic oxytocin neurones during bilateral and unilateral suckling in the rat. *Neurosci Lett* **227**, 17–20.

## Author contributions

I.R.P., L.A.M., A.F., S.D. and J.G.T. contributed to the conception and design of experiments, data collection and analysis, and the drafting of the article as well as revisiting it critically for important intellectual content. All authors have approved the final version of the manuscript. Y.U. made possible the identification of vasopressinergic cells through work in his laboratory at the University of Occupational and Environmental Health in Kitakyushu, Japan. Data were collected and analysed in the laboratory of J.G.T. at Tulane University in New Orleans, USA.

## Acknowledgements

We thank Professors William E. Armstrong and Robert C. Foehring for their generous contributions of time and space following hurricane Katrina. We thank Katalin Halmos for her immunohistochemistry and other expert technical assistance. We are indebted to Dr. Rebecca E. Green for her expertise in the art of Matlab programming. We thank Dr. Harold Gainer for the gift of antibody. This work was supported by NIH grant NS042081.